

Scaling of kinetic instability induced fast ion losses in NSTX

E.D. Fredrickson, D. Darrow, S. Medley, J. Menard, H. Park, L. Roquemore,
Princeton Plasma Physics Laboratory, Princeton, NJ
 D. Stutman, K. Tritz, *Johns Hopkins University, MD,*
 S. Kubota, *University of California, Los Angeles, CA.*
 K.C. Lee, *University of California, Davis, CA*

Introduction

A wide variety of fast ion driven instabilities are excited during neutral beam injection (NBI) in the National Spherical Torus Experiment (NSTX) by the large ratio of fast ion velocity to Alfvén velocity, together with the relatively high fast ion beta, β_f . The fast ion instabilities have frequencies ranging from the ion cyclotron frequency down to MHD frequencies. The modes can be divided roughly into three categories, starting with energetic particle modes (EPM) in the lowest frequency range (0 to 120 kHz), the Toroidal Alfvén Eigenmodes (TAE) in the intermediate frequency range (50 to 200 kHz) and the Compressional and Global Alfvén Eigenmodes (CAE and GAE, respectively) from ≈ 300 kHz up to the ion cyclotron frequency. Each of these categories of modes exhibits a wide range of behavior, including quasi-continuous behavior, bursting, chirping and, except for the lower frequency range (EPM), turbulence. Some examples of the range of EPM and TAE activity can be seen in Figs. 1a – 1c.

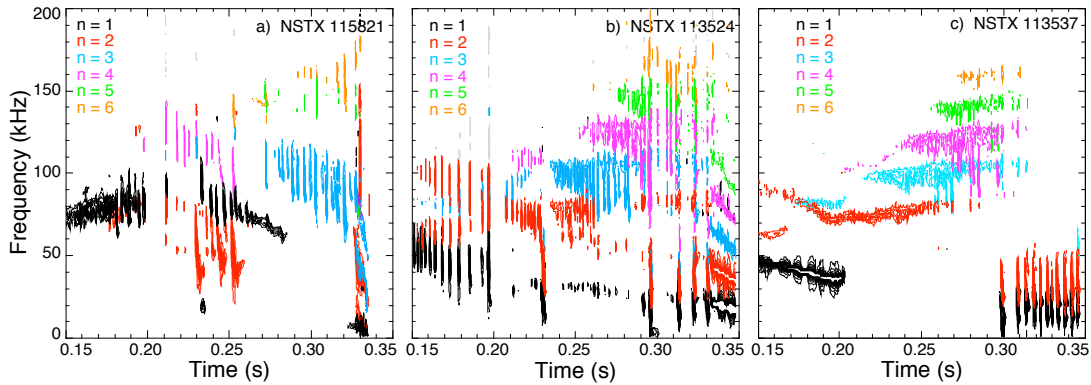


Fig. 1 Spectrogram of a Mirnov coil for three shots showing ‘low’ frequency fast ion driven instabilities, including Toroidal Alfvén Eigenmodes and various forms of Energetic Particle (chirping) Modes.

Fast ion driven modes are of particular interest because of their potential to cause transport, or even substantial losses, of fast ions. In NSTX beam heated plasmas we see transient neutron rate drops, correlated with bursts of fast ion driven instabilities, including modes identified as TAE and fishbone-like EPM [1]. The CAE and GAE may also affect fast ion confinement, but there is little direct evidence for enhanced transport of fast ions in the presence of these instabilities, and these modes will not be discussed further.

Fast ion loss events, together with TAE and EPM, are seen in nearly all regimes of NSTX NBI heated operation, up to the highest β_f , highest densities and at the highest plasma current, in contrast to the experience on MAST [2]. Fast-ion driven MHD activity can be reduced by operation at very high densities with low beam power, or with reduced beam voltage (<60 kV; typical injection energy is 80 kV), suggesting that the absence of TAE at high β_f on MAST is due to their lower voltage beams. On NSTX, EPM and TAE tend to be absent where $\beta_f(0)/\beta_{tot}(0) < 0.3$ (Fig. 2, green points).

Energetic Particle Modes

Energetic particle modes (EPM) are bursting modes where the frequency chirps down

strongly during each burst. The mode frequency can change rapidly because the frequency is determined by the fast-ion distribution function, which the mode can change on the mode growth timescale. On NSTX the EPM can have toroidal mode numbers from $n = 1$ up to at least $n = 5$. The EPM can be roughly divided into two groups, separated by the frequency range where they are found.

The high frequency EPM chirps start in the first shear-Alfvén gap, near the TAE frequency. These EPMs can have $n > 1$ and may be related to the rTAE [3], a TAE-like mode which can exhibit frequency chirping, or to the Infernal Fishbone [4]. The connection to the TAE can be seen in Figs. 1a-c where spectrograms of magnetic fluctuations are shown for three beam heated discharges. The energetic particle modes in the first shot (Fig. 1a) are discrete bursts with strong frequency chirping ($\Delta f \approx 50$ kHz). The bursts in the second example (Fig. 1b) are starting to overlap, and the frequency chirp weakens, but clearly starts at the TAE frequency. In the final example, the EPM appear as only intermittent chirps during quasi-continuous TAE activity.

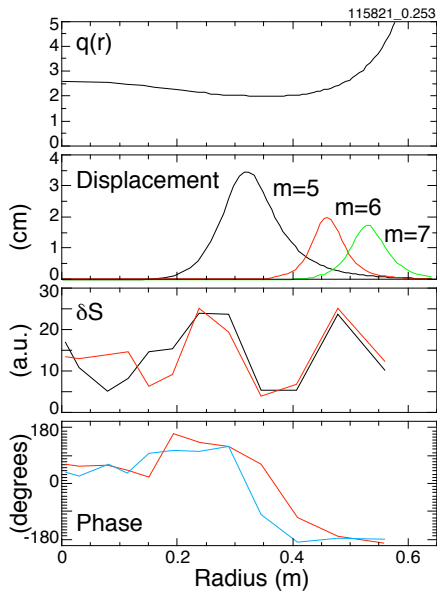


Fig. 3 Simulation of soft x-ray emissivity fluctuations for high frequency EPM. 2a) MSE/EFIT q-profile, 2b) trial eigenfunctions, 2c) simulated and measured soft x-ray chord integrated emissivity fluctuations, 2d) phase of simulated/measured fluctuations.

The MSE measurement of the q-profile indicates $q \approx 2$, similar to expectations for cascade modes, however the rate of the frequency chirp, the direction and the general characteristics of the frequency spectra are substantially different than what has been reported for cascade modes elsewhere [6]. It is possible that the energetic particle mode is

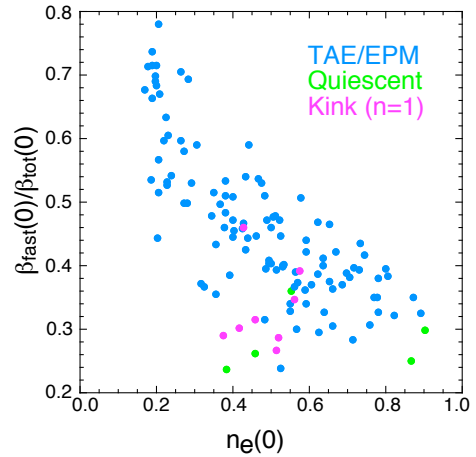


Fig. 2. Existence plot for TAE/EPM activity. EPM/TAE (green)

activity. EPM/TAE (green)

The large Doppler shift makes mode identification based on frequency ambiguous.

These higher frequency EPMs, as well as TAE, tend to be suppressed during low frequency EPM activity (Fig. 1b). The presence of high frequency EPMs appears to be correlated with elevated $q(0)$, or shear reversal, although the number of shots with MSE measurement of the q-profile is limited at this time.

The fast chirping suggests a non-linear resonant interaction similar to that for the conventional aspect ratio tokamak fishbone. However, the precession-drift frequency, the resonant interaction responsible for the fishbone chirp, is too low on NSTX to explain the high frequency of these EPMs. The resonance believed responsible for the high frequency EPMs is with the fast ion bounce frequency [5]. The bounce-resonance drive can be stronger at low aspect ratio in part because the average bounce angle is high. Thus, the hope that high β operation will suppress EPM by reducing or reversing the precession drift [1] is misguided.

responsible for suppression of the cascade modes.

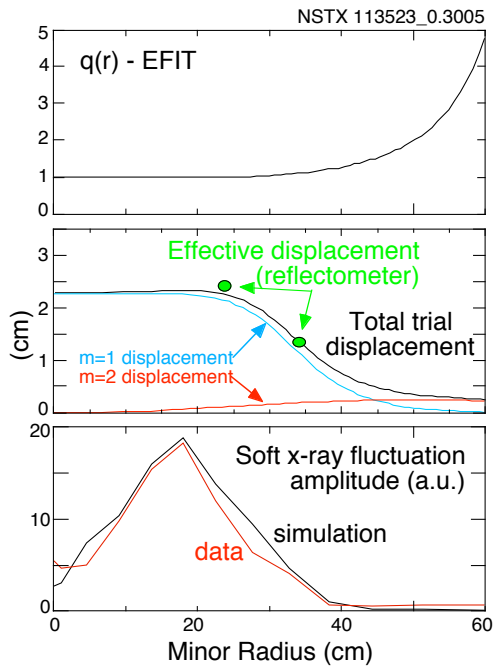


Fig. 4 Simulation of soft x-ray emissivity fluctuations for low frequency EPM. 2a) MSE/EFIT q -profile, 2b) trial eigenfunctions, 2c) simulated and measured soft x-ray chord integrated emissivity fluctuations

The low frequency EPM are similar to the fishbone modes on conventional tokamaks. They are present when $q(0) \approx 1$ (as calculated by EFIT), and have a kink-like structure. The soft x-ray camera data is well modeled with the assumption of an $m=1, n=1$ kink-like eigenfunction (Fig. 4), peaked on axis. The amplitude of the core displacement, which fits the soft x-ray data, is about 2.5 cm. In L-mode plasmas, with peaked core density profiles, the multi-channel heterodyne reflectometer can be used to measure the local mode displacement. For the mode shown in Fig. 4, the two reflectometer channels were fortuitously located near the minor radius of the inferred $q=1$ surface. The measured displacement agrees well with that inferred from the soft x-ray camera data.

Toroidal Alfvén Eigenmodes

Toroidal Alfvén Eigenmodes are seen in most operational regimes on NSTX, including shots with $\beta_{\text{tor}} > 35\%$. An example is shown in Fig. 5 from a shot which reached a peak toroidal β of $\approx 38\%$. The spectrum of TAE often appears incoherent or turbulent, with modes growing and decaying on a sub-millisecond timescale. In this example the $n=3$ and

The internal structure of the high frequency EPM has been studied in L-mode plasmas with soft x-ray data. The chord integrated soft x-ray emission can, in principle, be inverted with tomographic techniques. However, due to the limited number of chords, a better inversion can be made by introducing information from the time domain, as in rotational tomography. A further constraint on the inversion is to impose the equilibrium calculated from EFIT. The technique used is to assume the local soft x-ray emissivity is a flux surface quantity and perform a simple Abel-type inversion. A trial eigenfunction for the mode is introduced in a perturbative sense, and the soft x-ray chords are re-integrated and compared to the time behavior of the original data (Fig. 3). The simulations indicate that the peak mode displacement amplitude is ≈ 2.5 cm and probably localized near the q_{min} surface. However, the x-ray profile is hollow and sensitivity to mode structure is low in the core.

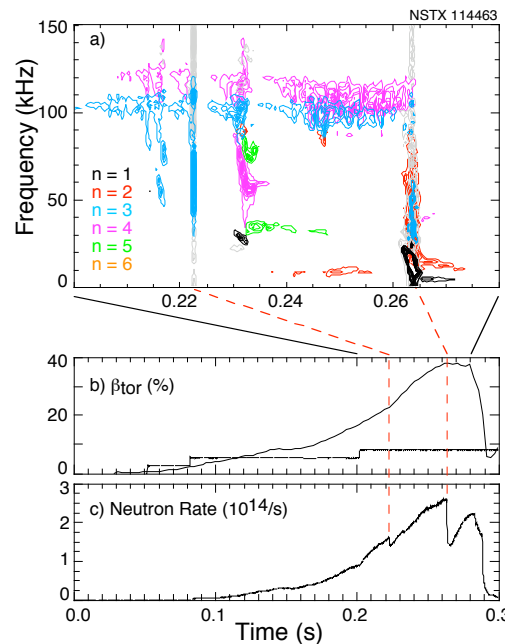


Fig. 5 Spectrogram showing TAE (and EPM) activity in high β NSTX plasma.

and

$n=4$ TAE were predominant. Several bursts of lower frequency chirping modes are also seen, and the two indicated resulted in substantial fast ion losses seen as abrupt neutron rate drops. All chirping events, however, were followed by a period of weaker TAE activity, suggesting that even though fast ions might not have been expelled from the plasma, there was redistribution in either real or velocity space.

Transient neutron drops, signifying fast ion loss events, are correlated with bursts consisting of multiple TAE. In Fig. 5 is shown an example where each burst includes at least five TAE with toroidal mode numbers $n = 2$ through 6. The strong drive for TAE, from the high fast ion beta, is hypothesized to drive TAE to sufficient amplitude such that there is overlap in phase space of the resonant interaction of fast ions with the TAE. Transport of fast ions in the presence of multiple, strongly driven TAE has been predicted for ITER.

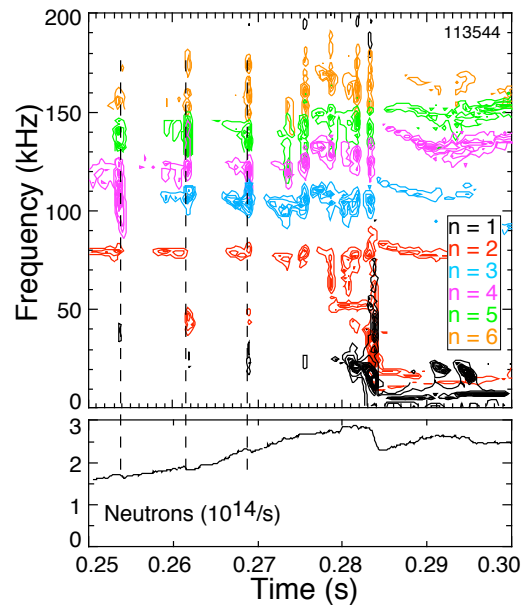


Fig. 6 Spectrogram of Mirnov coil showing correlation of burst of multiple TAE correlated with neutron drops.

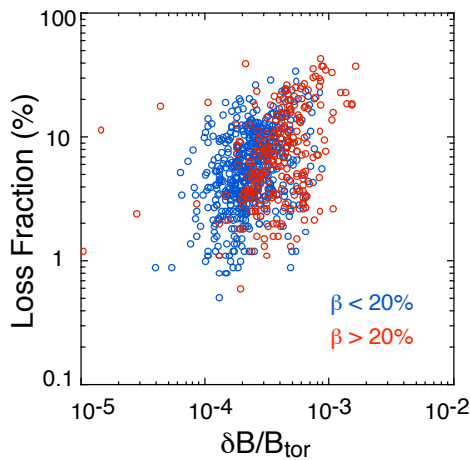


Fig. 6 Scaling of fast ion loss fraction with amplitude of EPM.

Scaling of losses

Fast ion loss events are most often correlated with chirping modes, either the low frequency fishbone-like modes, intermediate frequency EPs, or what appear to be weakly chirping, $\Delta f/f \leq 20\%$, TAE modes; possibly resonant TAE (rTAE). The neutron production is predominantly from beam-target interactions, so the fractional neutron rate drop is approximately the fast ion loss fraction. The fractional neutron rate drop scales loosely with the normalized amplitude of the energetic particle modes. The loss event data has been divided into those events occurring with $\Delta_{\text{tor}} < 20\%$ and $\Delta_{\text{tor}} > 20\%$. Fast ion loss events common at high and low beta.

This work is supported by U.S. DOE contract # DE-AC02-76CH03073.

References

- [1] E.D. Fredrickson, C.Z. Cheng, D. Darrow, *et al.*, Phys. of Plasmas **10** (2003) 2852.
- [2] M P Gryazneich and S E Sharapov, Plasma Phys. Control. Fusion **46** (2004) s15.
- [3] C.Z. Cheng and M.S. Chance, Phys. Fluids **29**, (1986) 2471.
- [4] Ya. I Kolesnichenko, VS Marchenko and R B White, PPPL Report PPPL-3786 (2003).
- [5] E D Fredrickson, L Chen, R B White, Nucl. Fusion **43** (2003) 1258.
- [6] S.E. Sharapov, B Alper, J Fessey, *et al.*, Phys. Rev. Lett. **93** (2004) 165001.